Therefore, instead of converting the model forest fires from a noncumulative to a cumulative distribution, we present the frequency-area data for actual forest fires in a noncumulative form. This could be done by binning the data. However, there would be ambiguities (for example, whether the bin size is in linear or logarithmic coordinates). Therefore, in order to compare the (noncumulative) model forest fire results with real forest fires, we converted a cumulative distribution of actual fire areas to a noncumulative one. We started with cumulative data, where $\dot{N}_{CF}$ is the number of forest fires per year with an area greater than A_F. We defined a noncumulative distribution in terms of the negative of the derivative of the cumulative distribution with respect to A_F. This value is negative because the cumulative distribution is summed from the largest to the smallest values. The derivative ($d\dot{N}_{CF}/dA_F$) is the slope of the best-fit line for a specified number of adjacent cumulative data points. Generally, we obtained excellent results using five adjacent points of the cumulative data and a least squares fit in linear space. The negative of each slope ($-d\dot{N}_{CF}/dA_F$) was plotted as a function of the average of the five adjacent log(A_F) points.

14. We thank J. Pelletier, A. Ruebel, J. G. Malamud, and J. Chiment for helpful suggestions and reviews of this manuscript. This research was supported by NASA grant NAGW-4072.

10 June 1998; accepted 7 August 1998

Molecular Assembly and Encapsulation Directed by Hydrogen-Bonding Preferences and the Filling of Space

Tomás Martín, Ulrike Obst, Julius Rebek Jr.*

Multiple copies of a molecule, held together in finite aggregates, give rise to properties and functions that are unique to their assembled states. Because these aggregates are held together by weak forces operating over short distances, a premium is placed on complementarity: The molecular surfaces must facilitate specific interactions that direct the assembly to one aggregate rather than another. Hydrogen-bonding preferences can be combined with molecular curvature to favor the assembly of four self-complementary subunits into a pseudo-spherical capsule. Filling the capsule with smaller, complementary molecules provides the final instruction for the assembly process.

Self-assembling systems highlight much of the current research in the chemistry of molecular recognition. The instructions for assembly are often written in the size, shape, and chemical surfaces of the interacting molecules. Hydrogen bonds, with their moderately directional characteristics and predictable patterns, are especially useful instructions, and their incorporation in molecules has resulted in a spectacular array of assemblies: Molecular ribbons (*1*), tapes (*2*), sheets (*3*), cages (*4*), rosettes (*5*), cubes (*6*), and capsules (*7*) have all been designed, synthesized, and characterized, both in solution and in the solid state. For the capsules, the formula has been the dimerization of self-complementary structures with appropriate curvature (*7, 8*). These result in assemblies that reversibly encapsulate smaller compounds to give "molecule-within-molecule" complexes (*9*). Here, we report the synthesis and characterization of a capsule composed of four identical subunits. We interpret its assembly and encapsulation behavior in terms of instruction in hydrogen bonding, molecular curvature, and the availability of suitable guest species.

Consider structure **1** as a candidate for assembly (Fig. 1A). At first glance, the presence of both H bond donors and acceptors in the molecule predicts some type of aggregation. However, the structure has particular contacts that suggest a specific array could form, as opposed to a less specific structure (*10*). First, the seven-membered ring adjacent to the glycoluril ring system at one end of the molecule and the α oxygen of the sulfamide at the other end impart a curvature to the structure: A cyclic array of molecules is probable (Fig. 1B). Second, the most acidic H bond donor (the sulfamide N-H) (*11*) is reasonably expected to pair with the most basic acceptor (the glycoluril carbonyl oxygen). These features can be expressed in a head-to-tail arrangement of four units in a macrocycle such as $\mathbf{1}_4$ (Fig. 1C) (*12*), in which all of the H bond donors find their complements—at nearly ideal distances and geometries—on nearest neighbors. Figure 1D shows the pattern of the 16 hydrogen bonds that hold the assembly together. This assembly creates a capsule with D_{2d} symmetry and a cavity for encapsulation of complementary guest molecules (Fig. 1E).

These notions were tested through the synthesis of compounds **1a** and **1b** (Fig. 2). For **1a**, 4,5-dimethyl-1,2-phenylenediamine **2** was converted into the cyclic sulfamide, then protected as its *t*-butyl carbamate (BOC group) to yield **3**. Benzylic dibromination of **3** gave **4**, which was coupled with the glycoluril building block **5a** (*13*) to yield **6**. Removal of the PMB (*p*-methoxybenzyl) and BOC protecting groups, using CAN (ceric ammonium nitrate) and CF_3CO_2H respectively, generated **1a**. The same synthetic scheme was followed to obtain monomer **1b**, which showed better solubility properties.

Subunit **1b** is readily soluble in dimethyl sulfoxide–d_6 (DMSO–d_6) (Fig. 3A) and other solvents that compete well for hydrogen bonds, and it exists in a monomeric state in

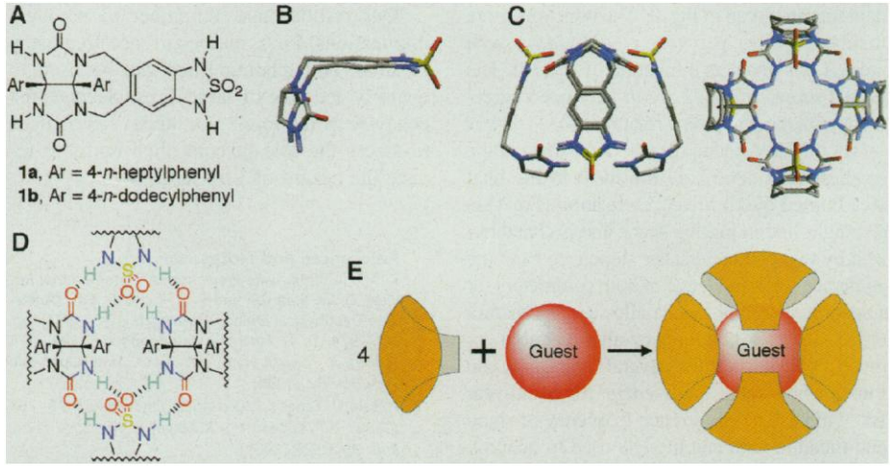

Fig. 1. (**A**) Structural depiction of monomers. (**B**) Side view of the monomer. (**C**) Molecular model (*12*) of the tetramer (atom colors: gray, carbon; dark blue, nitrogen; red, oxygen; light blue, hydrogen; yellow, sulfur). The aryl groups and some hydrogens have been omitted for clarity. (**D**) The pattern of hydrogen bonding in the assembly. (**E**) Schematic representation of the guest inducing the formation of a tetrameric assembly.

Skaggs Institute for Chemical Biology and Department of Chemistry, Scripps Research Institute, La Jolla, CA 92037, USA.

*To whom correspondence should be addressed.

those solvents. It is nearly insoluble in CD_2Cl_2 (Fig. 3B), $CDCl_3$, C_6D_6, toluene-d_8, and *p*-xylene-d_{10}. Nonetheless, after addition of adamantane derivatives **7** through **11** (Fig. 3) to CD_2Cl_2 suspensions of compound **1b**, new signals emerge in the nuclear magnetic resonance (NMR) spectra (Fig. 3, C to G) and the solid goes into solution. This solubility behavior is consistent with capsule assembly; the long alkyl chains of the glycoluril units are on the outer surface of the assembly where they interact with the bulk solvent, while the polar functionalities form intermolecular contacts that hold the system together.

The ^{1}H NMR data are consistent with assembly and encapsulation: The N-H resonances for the sulfamide and the glycoluril are shifted quite far downfield, and they are sharp and independent of concentration. The NMR assignments for the various N-H signals were confirmed through experiments with model compounds **12** and **13** (Fig. 4). The N-H signals of the sulfamide and urea in the tetramer $(\mathbf{1b})_4\cdot\mathbf{7}$ are at $\delta = 11.41$ ppm and $\delta = 5.92$ ppm, respectively (Fig. 3C), whereas the corresponding signals in the heterodimer **12**·**13** (see below) are at $\delta \sim 11.15$ ppm and $\delta \sim 5.99$ ppm. The new signals for encapsulated adamantane appear upfield; they are also sharp and widely separated from those of free adamantane ($\delta = 1.76$ ppm for the CH_2 of free adamantane, versus $\delta = 0.55$ ppm for the adamantane inside). These features speak for sizable energetic barriers between adamantanes in the bulk solvent and those in the new magnetic environment. The stoichiometry, obtained from integration of the spectra, shows roughly four molecules of compound **1b** per encapsulated adamantane. Accordingly, a highly ordered aggregate is formed: a pseudo-spherical molecular assembly with adamantane encapsulated as a guest. The exchange of guests in and out of the capsule is slow on the NMR time scale.

Adamantane has the shape and volume to fit in the capsule, but has only weak van der Waals interactions to offer the concave surface of the host's interior. Remarkably, this interaction is enough to overcome the entropic disadvantages involved in bringing five individual molecules into a highly ordered system. Moreover, adamantane competes successfully for the space of the capsule with the solvent CD_2Cl_2 (*14*). The tetrameric assembly can be further stabilized by the

Table 1. K_a(app) values and stoichiometry [equivalents of guest per equivalent of host tetramer (±10%)] for the encapsulation of guests in the tetramer $(\mathbf{1b})_4$. $\Delta G°$, free energies of formation in CD_2Cl_2 at 295 K (*17*, *18*).

Guest	Stoichiometry	K_a (M^{-1})*	$-\Delta G°$ (kcal mol^{-1})
7	1	19‡	1.7
8	1.1	48‡	2.3
9	1	160‡	3.0
10	1	3200§	4.7
11	–†	37‡	2.1

*These values are the average of three different measurements. †Value was not calculated because of the multiple signals of the guest. ‡Calculated by competition experiments (*18*). §Calculated by encapsulation experiments (*17*).

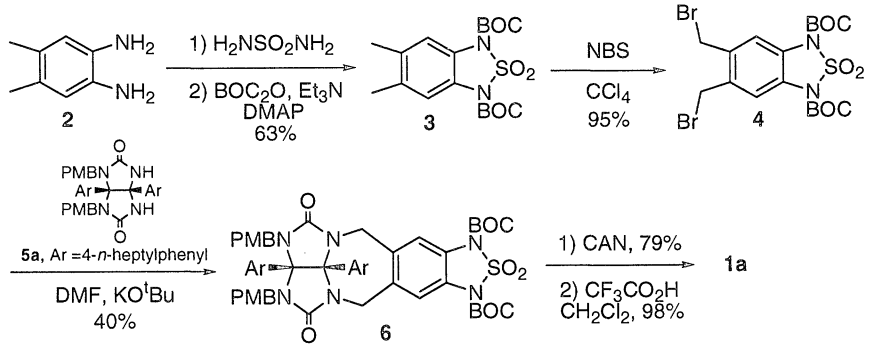

Fig. 2. Synthesis of monomer **1a**. Abbreviations: $(BOC)_2O$, di-*tert*-butyl dicarbonate; DMAP, 4-dimethylaminopyridine; BOC, *tert*-butoxycarbonyl; NBS, *N*-bromosuccinimide; DMF, *N*,*N*-dimethyl formamide; KO^{t}Bu, potassium *tert*-butoxide.

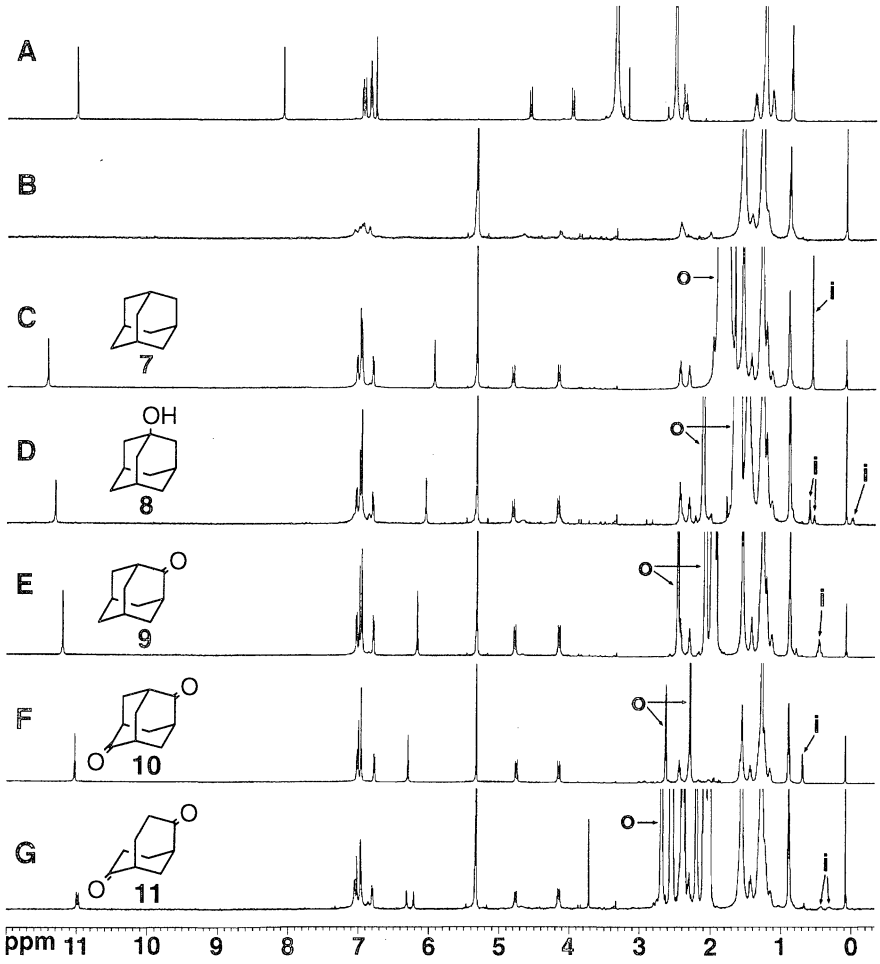

Fig. 3. ^{1}H NMR spectra (600 MHz) of **1b** (2.57 mM) in CD_2Cl_2 with guests **7** through **11**. The signals of the guest inside of the tetramer are labeled "i" and the signals of the guest outside, when resolved, are labeled "o." (**A**) Compound **1b** in DMSO-d_6. The signal at 2.5 ppm is from the solvent, and the signal at 3.3 ppm is H_2O. (**B**) Compound **1b** in CD_2Cl_2. The signal at 5.32 ppm is from the solvent, the signal at 1.55 ppm is H_2O, and the signal at 0.08 ppm is an impurity. (**C**) With excess adamantane (**7**). (**D**) With five equivalents of 1-adamantanol (**8**). (**E**) With five equivalents of 2-adamantanone (**9**). (**F**) With two equivalents of adamantane-2,6-dione (**10**). (**G**) With five equivalents of bicyclo[3.3.1]nonane-2,6-dione (**11**).

presence of H bond acceptor groups in the guest molecule through the formation of bifurcated H bonds with the glycoluril N-H groups of the capsule. Specifically, 2-adamantanone **9** and particularly adamantane-2,6-dione **10** (*15*) are very good guests: Less than 2 equivalents of **10** were required with respect to the monomer **1b** to give a homogeneous solution (Fig. 5). In the ^{1}H NMR spectrum of the tetrameric capsule $(\mathbf{1b})_4\cdot\mathbf{10}$ (Fig. 3F), we observe the signal for the encapsulated guest's CH_2 groups (8 H) at δ = 0.68 ppm, whereas the corresponding signal for the guest outside is at δ = 2.28 ppm.

Evidence for the formation of additional H bonds between guests containing carbonyl groups (**9**, **10**) and the capsule comes from the observed downfield shift of the glycoluril N-H groups with increasing number of guest carbonyl groups. The glycoluril N-H signal for the capsule with included adamantane (**7**, no carbonyl group) is located at δ = 5.93 ppm, whereas for the capsule containing **9** (one carbonyl group) δ = 6.17 ppm, and for guest **10** (two carbonyl groups) it shifts to δ = 6.33 ppm. At the same time, the N-H signals for the sulfamide group are shifted upfield: For the capsule occupied by **7** the signal is at δ = 11.41 ppm, for **9** it is at δ = 11.20 ppm, and for **10** it is at δ = 11.02 ppm. With chiral guests such as the diketone **11**, the capsule resonances are doubled (the N-H signals of the cyclic sulfamide are at δ = 10.99 ppm and 10.97 ppm, whereas the N-H signals of the glycoluril are at δ = 6.31 ppm and 6.21 ppm; Fig. 3G); symmetry axes are still present, but planes of symmetry are lost in the assembly (*16*). Although the presence of carbonyl groups in the guest increases its affinity for the capsule, filling the appropriate volume of the cavity appears to be the principal requirement for encapsulation. For example, 1,4-cyclohexanedione has carbonyl groups available for the H-bonding regions of the tetramer, but it is not encapsulated.

Because it was possible to observe and cleanly integrate the NMR signals of the guest **10** outside and inside of the tetramer, these data were used to calculate the equilibrium association constant (K_a) for the guest. The values are here denoted as apparent association constants, K_a(app), because of the simplification of several dynamic processes (*17*). The reliable K_a(app) for **10** was then used to calculate constants for the other guests through direct competition experiments (Table 1) (*18*).

The H-bonding preferences in these assemblies are reasonable, but additional experiments were carried out using the urea **12** and the sulfamide **13** (*19*) to test whether the association between ureas and cyclic sulfamides is general. Dilution experiments performed with the individual compounds and with a 1:1 mixture of both (Fig. 4) showed that heterodimerization (**12·13**) is indeed preferred to homodimerization (**12·12** and **13·13**, respectively). Thus, a cyclic sulfamide is potentially a useful building block for the construction of other three-dimensional assemblies.

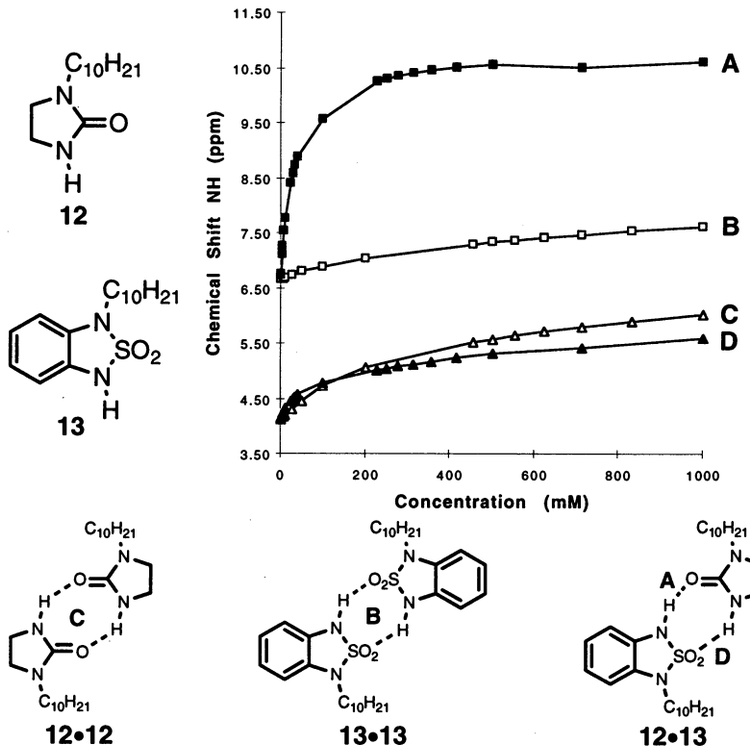

Fig. 4. Dilution experiments in CD_2Cl_2 of the compounds **12** and **13** and their 1:1 mixture. The heterodimer **12·13** shows greater stability than either of the homodimers (**12·12** and **13·13**), as shown by the NMR chemical shifts for the protons labeled **A** through **D**.

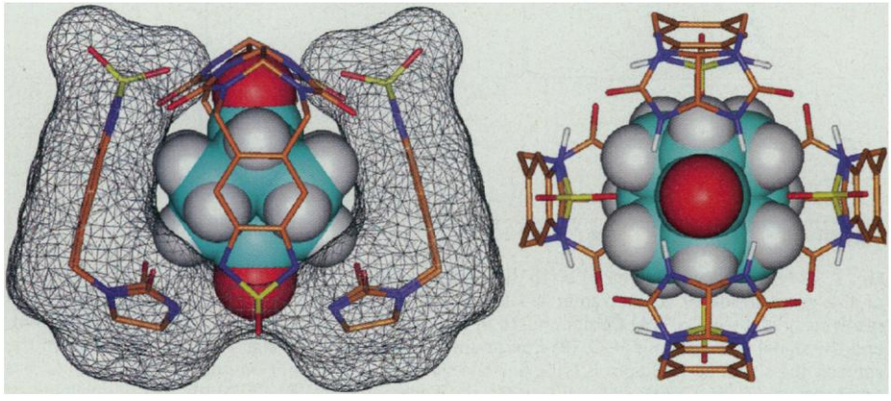

Fig. 5. Two views of the tetrameric capsule filled with **10** obtained by modeling (*12*). The aryl groups and some hydrogens have been omitted for clarity.

References and Notes

1. M. Gallant, M. T. P. Viet, J. D. Wuest, *J. Org. Chem.* **56**, 2284 (1991); F. Garcia-Tellado, S. J. Geib, S. Goswami, A. D. Hamilton, *J. Am. Chem. Soc.* **113**, 9265 (1991).
2. J. A. Zerkowski, C. T. Seto, D. A. Wierda, G. M. Whitesides, *J. Am. Chem. Soc.* **112**, 9025 (1990); J. A. Zerkowski, C. T. Seto, G. M. Whitesides, *ibid.* **114**, 5473 (1992); J. A. Zerkowski, J. C. MacDonald, C. T. Seto, D. A. Wierda, G. M. Whitesides, *ibid.* **116**, 2382 (1994).
3. L. Leiserowitz and G. M. J. Schmidt, *J. Chem. Soc. A*, (1969), p. 2372; K. D. M. Harris and M. D. Hollingsworth, *Nature* **341**, 19 (1989); Y.-L. Chang, M.-A. West, F. W. Fowler, J. W. Lauher, *J. Am. Chem. Soc.* **115**, 5991 (1993).
4. C. M. Drain, R. Fischer, E. G. Nolen, J.-M. Lehn, *J. Chem. Soc. Chem. Commun.* **1993**, 243 (1993).
5. G. M. Whitesides, J. P. Mathias, C. T. Seto, *Science* **254**, 1312 (1991); S. C. Zimmerman, F. Zeng, D. E. C. Reichert, S. V. Kolotuchin, *ibid.* **271**, 1095 (1996); R. H. Vreekamp, J. P. M. van Duynhoven, M. Hubert, W. Verboom, D. N. Reinhoudt, *Angew. Chem. Int. Ed. Engl.* **35**, 1215 (1996); J. Yang, J.-L. Marendaz, S. J. Geib, A. D. Hamilton, *Tetrahedron Lett.* **35**, 3665 (1994).
6. L. R. MacGillivray and J. L. Atwood, *Nature* **389**, 469 (1997).

7. M. M. Conn and J. Rebek Jr., *Chem. Rev.* **97**, 1647 (1997) and references therein.
8. R. G. Chapman and J. C. Sherman, *J. Am. Chem. Soc.* **117**, 9081 (1995).
9. For covalently bound "molecule-within-molecule" complexes, see D. J. Cram and J. M. Cram, *Container Molecules and Their Guests* (Royal Society of Chemistry, Cambridge, 1994).
10. In an earlier attempt to bring together four identical molecules into a self-assembled tetramer, urea functions were used as the exclusive hydrogen-bonding units, but this formed an extended ribbon structure in the solid state [X. Garcías, L. M. Toledo, J. Rebek Jr., *Tetrahedron Lett.* **36**, 8535 (1995)]. For a planar tetrameric assembly related to G-quartets, see R. G. Barr and T. J. Pinnavaia, *J. Chem. Phys.* **90**, 328 (1986).
11. P. O. Burke, S. D. McDermott, T. J. Hannigan, W. J. Spillane, *J. Chem. Soc. Perkin Trans.* **2**, 1851 (1984).
12. Molecular modeling was performed using Macromodel 5.5 (Amber* force field) [F. Mohamadi *et al.*, *J. Comput. Chem.* **11**, 440 (1990)]. The positions of the sulfamide hydrogens were assumed to be time-averaged in the plane of the aromatic ring.
13. D. M. Rudkevich and J. Rebek Jr., *Angew. Chem. Int. Ed. Engl.* **36**, 846 (1997).
14. S. Mecozzi and J. Rebek Jr., *Chem. Eur. J.* **4**, 1016 (1998).
15. C. Morat and A. Rassat, *Tetrahedron Lett.* **45**, 4409 (1979).
16. Y. Tokunaga and J. Rebek Jr., *J. Am. Chem. Soc.* **120**, 66 (1998).
17. For the calculation of apparent association constants, we used the integration of peaks of the guest inside and outside of the capsule that were obtained by ^{1}H NMR. There is an estimated 10% error in these measurements. The equilibrium can be described as follows:

$$H_{aggregate} + G \overset{K_a(app)}{\rightleftharpoons} H_4G$$

The following assumptions were made: (i) the amount of tetramer (unfilled or filled with solvent) present before addition of the guest is negligible; (ii) after addition of the guest, all of the host material not assembled into the capsule (including solid material) is in the aggregate state; and (iii) the association of the guest with itself is negligible.

$$K_a(app) = \frac{[H_4G]}{[H_{aggregate}][G]} = \frac{xV}{(h - x)(g - x)}$$

$$\Delta G° = -RT \ln K_a(app)$$

$$x = g(I_{gi}/I_{gt})$$

$$I_{gt} = I_{go} + I_{gi}$$

In these equations, $H_{aggregate}$ is the host as a low-ordered aggregate, G is the guest, H_4G is the tetramer complex, x is the amount of guest (in millimoles) in the complex H_4G, V is the total volume (in milliliters), h is the initial theoretical amount of tetramer (in millimoles), g is the amount of guest (in millimoles) added to the solution, $\Delta G°$ is the free energy of formation, R is the ideal gas constant, T is temperature (kelvin), I_{gt} is the sum of all the integrals corresponding to the guest, I_{go} is the integral for the signal of the guest outside of the tetramer complex, and I_{gi} is the integral for the signal of the guest inside of the tetramer complex. To obtain K_a(app) for guest **10**, we added 0.5 equivalents of the guest with respect to the monomer **1b** in CD_2Cl_2, sonicated the heterogeneous solution for 30 min, and measured the ^{1}H NMR spectrum after 30 hours.
18. The competition experiments were performed by the addition of different amounts of one guest (G′) to compound **1b** with another guest (G) present. The ratio of the two complexes H_4G and H_4G' was obtained by integration of the N-H signals of the two species. The equilibrium may be described as follows:

$$H_4G + G' \overset{K}{\rightleftharpoons} H_4G' + G$$

$$K = \frac{[H_4G'][G]}{[H_4G][G']} = \frac{K_a'(app)}{K_a(app)}$$

19. These compounds were prepared by monoalkylation of the corresponding urea and cyclic sulfamide with 1-bromodecane. The presence of the long alkyl chain is necessary for good solubility in noncompetitive solvents.

20. Supported by NIH and the Skaggs Research Foundation. T.M. thanks the Ministerio de Educación y Cultura of Spain for providing postdoctoral fellowship support. U.O. thanks the Deutsche Forschungsgemeinschaft for a postdoctoral fellowship.

4 June 1998; accepted 12 August 1998

Inhibition of Xenoreactive Natural Antibody Production by Retroviral Gene Therapy

Jennifer L. Bracy, David H. Sachs, John Iacomini*

The major barrier to transplantation across discordant species, such as from pig to human, is rejection mediated by xenoreactive natural antibodies (XNA) that bind the carbohydrate epitope Galα1-3Galβ1-4GlcNAc-R (αGal) on donor tissues. This epitope is synthesized by the enzyme glucosyltransferase uridine 5′-diphosphate galactose:β-D-galactosyl-1,4-*N*-acetyl-D-glucosaminide α(1-3)galactosyltransferase (E.C. 2.4.1.151), or simply αGT. When a functional αGT gene was introduced by retroviral gene transfer into bone marrow cells, αGal XNA production in a murine model ceased. Thus, genetic engineering of bone marrow may overcome humoral rejection of discordant xenografts and may be useful for inducing B cell tolerance.

A shortage of human organs has stimulated a great deal of research into the possibility of using nonhuman donors for transplantation. Pigs are the most likely species to serve as donors for clinical xenotransplantation because of their similarity to humans (*1, 2*). However, humoral rejection mediated by αGal XNA remains a major barrier to successful xenotransplantation (*3, 4*). Although several approaches have been developed to prevent hyperacute rejection mediated by αGal XNA, delayed rejection caused by these antibodies remains a formidable challenge (*5–8*). For xenotransplantation to be successful, methods must be developed to overcome organ damage mediated by αGal XNA.

Induction of mixed chimerism by bone marrow transplantation can be used to tolerize B cells producing αGal XNA (*9*), but this is not a practical solution (*10*). We hypothesized that production of αGal XNA may be inhibited by introducing a functional αGT gene by retroviral gene transfer into autologous bone marrow cells. αGal epitopes would then be expressed on the surface of bone marrow–derived cells or on secreted proteins that could potentially tolerize B cells making αGal XNA. Thus, establishing molecular rather than cellular chimerism could circumvent difficulties associated with engraftment of pig bone marrow in primates for the purpose of inducing tolerance.

To construct a retroviral vector (*11*) carrying the gene encoding porcine αGT, we isolated from the plasmid pSal3GT1 an 1145–base pair (bp) Eco RI–Cac 8I DNA fragment containing the coding region of pig αGT (*12*) and cloned it together with the murine phosphoglycerate kinase promoter into the N2A retroviral vector (*13*) to construct LGTRV (Fig. 1A). The LGTRV construct was transfected into the amphotropic retroviral packaging cell line AM12 (*14*) to derive the virus producer cell line LGTA7. The viral titer of supernatants harvested from the LGTA7 line was approximately 5×10^4 to 1×10^5 colony-forming units per milliliter. To test whether LGTA7-derived virus could transfer functional αGT expression, we transduced Vero cells with LGTA7 or a control virus containing only the neomycin resistance (neo^r) gene, and surface expression of αGal epitopes was analyzed by staining with the isolectin BSI-B_4 (IB4 lectin) isolated from *Bandeiraea simplicifolia*, which specifically binds αGal (*15*). G418-resistant Vero cell clones infected with LGTA7 expressed αGal epitopes on the cell surface at levels detectable by staining with IB4 lectin (Fig. 1B). Surface expression of αGal epitopes was stable and could be detected on the surface of transduced cells for at least 4 months in culture. In contrast, no surface expression of αGal epitopes was detected on Vero cells transduced with control virus. Treatment of LGTA7-transduced Vero cell clones

J. L. Bracy, Cellular and Molecular Biology Program, Allegheny University of the Health Sciences, 2900 Queen Lane, Philadelphia, PA 19129, USA, and Transplantation Biology Research Center, Massachusetts General Hospital and Harvard Medical School, Building 149-5210, 13th Street, Boston, MA 02129, USA. D. H. Sachs and J. Iacomini, Transplantation Biology Research Center, Massachusetts General Hospital and Harvard Medical School, Building 149-5210, 13th Street, Boston, MA 02129, USA.

*To whom correspondence should be addressed. E-mail: iacomini@helix.mgh.harvard.edu